Vertical diffusivity in the lower stratosphere from Lagrangian back-trajectory reconstructions of ozone profiles

B. Legras[1], B. Joseph[1,3], F. Lefèvre[2]

Abstract. We present a simple stochastic-dynamical approach to estimate the turbulent vertical diffusivity (D) in the lower stratosphere from routinely observed ozone profiles. First, an observed ozone profile is reconstructed using three-dimensional back-trajectories obtained from analyzed winds and initializing the trajectories with ozone values from the output of a chemistry-transport model. Assuming that diffusion in the vertical follows a simple random walk leading to a Gaussian probability distribution for the particle displacements, we perform Monte-Carlo simulations with ensembles of particles originating along each point in the vertical profile. By choosing different values of D as input in the calculations, we generate different profiles that are smoothed through diffusion. Comparing with the observed profile, we can identify that value of D which is in best agreement at an intermediate range of vertical length scales as an upper bound of the actual D. For northern mid-latitude lower stratospheric conditions during winter over a period of 12 days, the best estimate is $D \approx 0.1 \mathrm{m^2 s^{-1}}$or slightly larger. The present results are discussed in the context of comparable estimations of vertical diffusivity in the literature.

1. Introduction

Vertical diffusivity (D) is a crucial parameter in Eulerian models of tracer transport. Eulerian numerical models, often, use an eddy diffusivity parameterization of small-scale vertical mixing which is analogous to Fickian (ordinary) diffusion, with a diffusivity which is several orders of magnitude greater than the molecular diffusion coefficient (10^{-4} $\mathrm{m^2 s^{-1}}$in the lower stratosphere). It may be argued that the overall effect of vertical transport by the action of inhomogeneously distributed mixing (turbulent) layers in stratified flows, such as in the stratosphere, may be represented by an ordinary diffusion process in the vertical, even though such individual mixing events can be strongly intermittent and patchy in space and time [*Dewan*, 1981; *Vanneste and Haynes*, 2000]. However, the literature exhibits a variety of estimates for a representative value of the vertical diffusion to be used in numerical models.

Early observational estimation of D in the lower stratosphere had mostly been based on turbulence characteristics deduced from radar measurements, and values of D in such studies are roughly in the range 0.1 to 1.0 $\mathrm{m^2 s^{-1}}$[*Woodman and Rastogi*, 1984; *Fukao et al.*, 1994; *Nastrom and Eaton*, 1997]. Numerical estimates from idealized mesoscale model simulations suggested that vertical diffusivity in the above range can be realized by short time-scale (last a few hours) individual events of dynamical (Kelvin-Helmholtz) instabilities or breaking gravity waves in the lower stratosphere [*Schilling and Jenssen*, 1992; *Schilling and Etling*, 1996]. However, recent modeling studies using high resolution, lower stratospheric balloon data give values of D, valid for a lifetime of few hours, in the range 0.01 - 0.02 $\mathrm{m^2 s^{-1}}$[*Alisse et al.*, 2000]. Similar values are also deduced from recent radar measurements [*Dole and Wilson*, 2000] using a somewhat ad hoc intermittency factor. Other studies have deduced about the values of D from high resolution tracer data from aircraft campaigns, assuming that observed distribution of tracers arises from a combination of large-scale advective stirring and mixing effects due to turbulence [*Waugh et al.*, 1997; *Balluch and Haynes*, 1997]. These estimates of D, valid over 1 to 2 weeks, are of the order of 0.01 $\mathrm{m^2 s^{-1}}$or even lesser. It is also interesting to notice that combined effect of mean (diabatic) Brewer-Dobson circulation and quasi-horizontal stirring by large eddies, in the absence of small-scale turbulence, are found to result in a transport that can be represented by a diffusivity D of about 0.2 $\mathrm{m^2 s^{-1}}$, on time scales of a month or more in the mid-latitude surf zone [*Sparling et al.*, 1997].

The standard phenomenology of turbulent dispersion in two and three dimensions [*Richardson*, 1926; *Taylor*, 1921; *Morikawa and Swenson*, 1971; *Zouari and Babiano*, 1994] suggests that diffusion value increases monotonically as a function of spatial and temporal scales and saturates in a Brownian asymptotics at large scale. The large values obtained from the radar measurements are clearly inconsistent with this simple view. The discrepancy is usually attributed to the role of intermittency in the turbulent scales [*Alisse et al.*, 2000; *Dole and Wilson*, 2000].

Both estimates of *Waugh et al.* [1997] and *Balluch and Haynes* [1997] were based on the dominating layer-wise motion in the stratosphere to generate filaments of tracers. By reconstructing the filaments with high resolution and comparing with airborne observations *Waugh et al.* [1997] found

[1]Laboratoire de Météorologie Dynamique (UMR 8539), Paris
[2]Service d'Aéronomie (UMR 7620), Paris
[3]Dept of Mathematics, Arizona State Univ., Tempe

Paper number .
0148-0227/03/$9.00

a bound on the horizontal diffusion that was converted to a vertical diffusion by further estimating the aspect ratio of the structures from the ratio of horizontal strain to vertical shear. *Balluch and Haynes* [1997] estimated an upper bound on vertical diffusivity by studying the evolution of single filaments submitted to horizontal strain and vertical shear. In this study, we present a complementary approach which estimates D in the lower stratosphere from the comparison of observed ozone profiles in the mid-latitudes with stochastic-dynamical reconstructions.

Reconstructions of small-scale tracer structures are done with a variety of Lagrangian techniques among which reverse domain filling back trajectories (RDF) and contour advection (CA) are the most commonly used [*Sutton et al.*, 1994; *Waugh et al.*, 1994]. Most of the applications of these Lagrangian reconstruction techniques have been limited to two-dimensional advection along isentropic surfaces, due to its physical validity for a week or so with diabatic heating/cooling of the order of 1 K/day in the lower extratropical stratosphere. Vertical tracer profiles are obtained by multi-layer CA or by RDF in a vertical plane. The reconstructed profiles exhibit laminae which are the vertical trace of the sloping filaments seen in the isentropic maps and often corresponds to similar structures seen in the observed soundings [*Orsolini*, 1995; *Mariotti et al.*, 1997; *Orsolini et al.*, 2001]. However, when a large number of vertical levels are used in the reconstruction, we shall see below that the density of laminae in the reconstructed profile largely exceeds the observed number of similar structures in high-resolution in-situ profile. This is a sign that the chaotic cascade in the reconstructed field is not halted by three-dimensional mixing as in the atmosphere. By introducing a numerical vertical diffusion, and increasing it until it fits the observed profile (we shall be more precise about this fit later), we obtain an estimate of the vertical diffusion in the atmosphere.

One of the difficulties in comparing tracer reconstruction with observations is that the common choice for the reconstructed quantity is the potential vorticity (PV). PV is usually conserved within the stratosphere for one week or two and is available on a global scale as operational analyses data from weather centers. Thus it provides a convenient way to initialize the reconstructions. However, high-resolution in situ measurements are for chemical compounds like ozone, not PV. The existence of a statistical relation between PV and ozone is an unreliable tool to interpret the details of a given reconstructed profile because the relation is only true on the average and allows large local fluctuations depending of the dynamical and chemical history of fluid parcels. It is therefore desirable to perform the reconstructions directly on ozone fields, which leads to the problem of finding adequate ozone data for the initialization. Over the recent years, there was no satellite instrument providing a global coverage of the three-dimensional distribution of ozone. This is why we have used the ozone fields from a chemical transport model in order to initialize our integrations.

2. Data and methods

The observed ozone profiles to be used as a reference in our comparisons are those from ground-based ozonesonde measurements in the northern mid-latitudes, available from Norwegian Institute for Air Research (NILU) during the winter of 1998-99. The sounding data are available with an average frequency of 0.25 Hz, corresponding to a mean vertical resolution of about 25 m. The instrumental response of the chemical cell further limits the practical vertical resolution to perhaps 100 m. We use a selected interval of the profiles spanning the tropopause and the lower stratosphere. In the first part of section 3 the profiles are interpolated, using Akima method *Akima* [1991], to 241 points regularly distributed in z over the selected interval 12-24 km, while in the rest of the study the same method is used to interpolate to 500 points regularly distributed in log-pressure over the interval 180-25 hPa. The results are only weakly sensitive to this procedure.

The trajectory reconstructions utilize the European Centre for Medium-Range Weather Forecast (ECMWF) 3-hourly winds truncated at a resolution T106 and projected onto a $1\,\mathrm{deg} \times 1\,\mathrm{deg}$ grid in latitude and longitude [1]. The wind fields are avalaible on the hybrid ECMWF levels. There are 31 levels between the ground and 10 hPa for December 1998 and January 1999, and 50 levels between the ground and 0.1 hPa for March 1999. Back trajectories are computed with FLEXPART-ST, a modified and optimized version of the FLEXPART trajectory code available from Andreas Stohl at the University of Munich [*Stohl et al.*, 2002; *James et al.*, 2002] using a fixed time-step of $\delta t = 900$ s. The wind is linearly interpolated in time, longitude, latitude and log-pressure at the location of the particles in time and space. The ozone values of back trajectories are initialized from the global ozone fields output of the REPROBUS (REactive Processes Ruling the Ozone BUdget in the Stratosphere) CTM (Chemistry Transport Model) [*Lefèvre et al.*, 1994]. Because the number of available fields from REPROBUS was limited, this has reduced the number of usable soundings during this study. Four cases chosen in December 1998, January and March 1999 have been investigated.

REPROBUS is a three-dimensional chemical transport model (CTM) with a comprehensive treatment of gas-phase and heterogeneous chemical processes in the stratosphere [*Lefèvre et al.*, 1994, 1998]. Long lived species, including ozone, are transported by a semi-Lagrangian scheme [*Williamson*, 1989] forced by the 6-hourly ECMWF wind analysis. For the experiments presented here the model was integrated with a horizontal resolution of $2\,\mathrm{deg} \times 2\,\mathrm{deg}$. The REPROBUS ozone profiles shown for December 1998 were obtained with a 31-level version of the model identical to the ECMWF analysis. This run was initialized on 30 November 1998. The January and March 1999 profiles are the results of a different simulation starting on 1 January 1999, which takes advantage of a pre-operational 50-level ECMWF analysis extending up to 0.1 hPa with a significantly improved vertical resolution in the lower stratosphere. The REPROBUS output are available on the 38 upper levels of the ECMWF analysis. For both simulations the three-dimensional initial ozone field was reconstructed by using the ozone-PV correlation derived from the measurements of the POAM III (high and mid-latitude air) and HALOE (tropical air) satellite instruments [*Lucke et al.*, 1999; *Bhatt et al.*, 1999]

The deterministic Lagrangian reconstruction method used in this study is as follows. Along the lower stratospheric segment of an observed ozone profile, we initialize an ensemble of N particles equally distributed in altitude or log-pressure coordinate over an interval (between 12 km

and 24 km or between 180 hPa and 25 hPa) spanning the tropopause and the lower stratosphere. Then, back trajectories for 10 to 24 days, depending on the availability of the REPROBUS fields, are computed using FLEXPART-ST. The final locations of the back trajectories are then used to prescribe the ozone mixing ratio of the advected parcel using the output of REPROBUS at this date. Assuming that ozone is advected passively during the reconstruction time-period, the ozone values obtained from this initialization are attributed to the initial location of particles on the initial profile. A similar method was used by *Orsolini et al.* [2001] using MLS observations to reconstruct ozone lidar profiles.

The reconstruction can be done either by assuming isentropic trajectories, by which the potential temperature θ is conserved during the motion, or by using the full three-dimensional velocity from ECMWF analysis[2]. In both cases, we assume that the ozone mixing ratio C is conserved during the motion. This is justified by the fact that fast small-scale motions, which are responsible of the vertical mixing, are absent from the dataset.

In order to represent the small-scale vertical mixing we add to our model a stochastic component such that the parcel motion over a small time interval δt is given by

$$\delta \mathbf{X} = \mathbf{V}(\mathbf{X}, t)\delta t + \delta\eta(t)\mathbf{k} \tag{1}$$

where $\delta\eta(t) \equiv w\delta t$ is a white noise process for the vertical motion and $\mathbf{k}$ is the vertical unit vector. This process is without memory (i.e. it is δ-correlated in time), and with a zero mean. If the limit $\delta t \to 0$ and after statistical average over a large number of particles, this is equivalent to adding a diffusion to transport such that C is no longer conserved. That is

$$\frac{\partial C}{\partial t} + \mathbf{V}\cdot\nabla C = D\frac{\partial^2 C}{\partial z^2}\,, \tag{2}$$

with

$$D = \frac{1}{2} < w^2 > \delta t\,. \tag{3}$$

In order to ensure that vertical velocities are bounded, we use a white noise based on a random variable r that is uniformly distributed over the interval $[-\sqrt{3}, \sqrt{3}]$ with zero mean and unit variance. Applying (3), the random process is then $\delta\eta = r\sqrt{2D\delta t}$ with a new drawing of r at each time step and for each particle.

Since FLEXPART-ST is formulated in vertical log-pressure coordinate z^*, the random vertical displacement is given as

$$\delta z^* = \frac{g}{RT}\delta\eta\,. \tag{4}$$

In a stratified fluid where vertical motion is inhibited by the potential temperature gradient, a natural alternative to the diffusion in z is to model vertical mixing as a diffusion in θ-coordinate. In this case, $\delta\eta$ is considered as a motion in θ coordinate, and (2) is replaced by

$$\frac{\partial C}{\partial t} + \mathbf{V}\cdot\nabla C = D_\theta\frac{\partial^2 C}{\partial \theta^2}\,.$$

The random vertical displacement is now

$$\delta z^* = \left(\frac{p}{p_0}\right)^\kappa \left(\kappa T - p\frac{dT}{dp}\right)^{-1}\delta\eta\,. \tag{5}$$

The number of particles launched from a single point on the profile for a diffusive reconstruction is $M = 4000$. With $N = 500$, 2×10^6 trajectories are initialized along each lower stratospheric segment of the ozone profile and integrated backward in time using (1). The reconstructed ozone value on the profile is the average mixing ratio of the M particles arriving at each point. Because of this finite sampling of the Gaussian diffusive probability distribution of particles, an additional spurious stationary random process with variance proportional to D/M and a white spectrum is introduced in the process. It is seen below that this particle noise is visible only for the largest value of D we have investigated.

3. Results

First, we present the deterministic reconstructions of ozone profiles in order to exemplify certain advantages of the Lagrangian approach when simulated profiles are to be compared with observed ones. Then, we focus on the main aim of this work that is to estimate the vertical diffusivity in the lower stratosphere.

Figure 1 shows the four selected ozone profiles in the northern mid-latitudes obtained during the THESEO campaign in the winter 1998-99. In each panel, the observed profile is compared to the REPROBUS profile and reconstructed profiles with N=241 using isentropic and three-dimensional (3D) trajectories over 8 to 9 days. It is clear that REPROBUS, even though successful in capturing the general trends in the observed profiles, does not capture the small-scale variability. The passive advection of particles along trajectories generates small-scale structures in the reconstructed profile and reproduces some of the observed features missing in the REPROBUS profile. However, fluctuations in the Lagrangian reconstructed profiles are much too large compared with the observations. It is by eliminating this artifact that we are able to estimate the vertical diffusion due to small-scale unresolved motion.

Figure 1(a-c) shows typical examples for which the reconstructed ozone profiles in the lower stratosphere are relatively independent of whether advection is done using isentropic or three-dimensional winds, over a period of 9 days. This illustrates the validity of the adiabatic assumption over such a period. However, as evident from Figure 1(d), there are also instances where diabatic effects is important, at least in the ECMWF analysis. Here a strong descent occurs from about 450 K upwards, of the order of 5 K/day near 500 K, which clearly means that diabatic processes cannot be neglected. This cooling is compatible with the response to the major stratospheric warming of mid-December 1998 [*Manney et al.*, 1999]. The isentropic reconstruction is, however, in better agreement with the observed than the 3D reconstruction or the REPROBUS curve (which depends also on the ECMWF analysed winds). This leads us to conjecture that the analysis overestimates the diabatic cooling or that its geographical distribution wrongly encompasses the region traversed by air parcels sampled in the Legionowo profile. Another, admittedly less likely, hypothesis is that the analysed cooling is correct, but that the Legionowo profile samples air having experienced significant ozone depletion during the prevailing cold conditions of the first half of December 1998 [*European Ozone Research Coordinating Unit*, 1999; *Millard et al.*, 2002]. It appears that Lagrangian

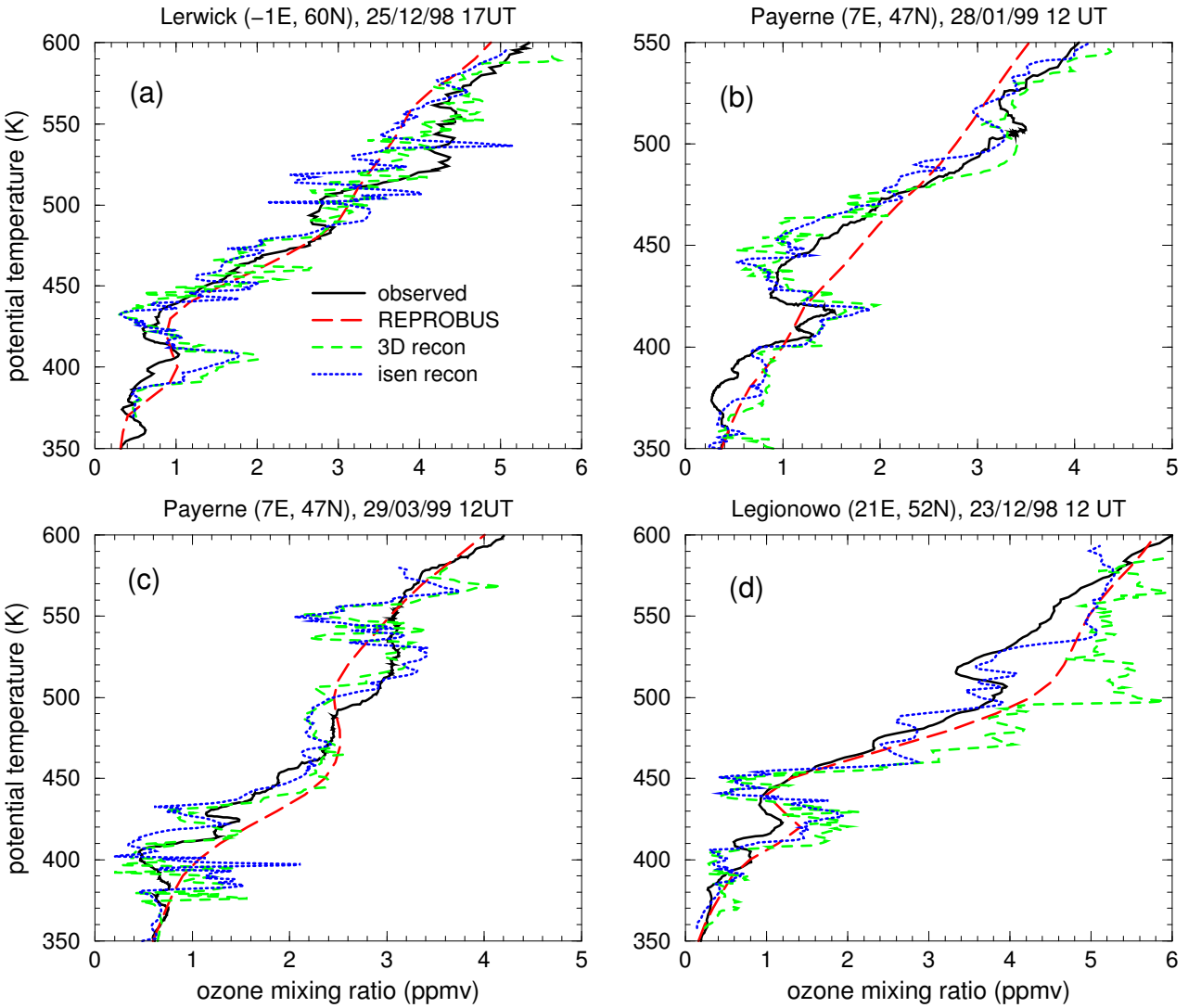

Figure 1. Ozone profiles at various stations and times combining observed data, interpolated REPROBUS data, isentropic and 3D reconstructions, as indicated in the titles and legends. The number of points in the profiles is $N = 241$. They are equally distributed every 50 m between 12 km and 24 km. Trajectories have been integrated backward in time until (a) 17 December 1998 at 12 UT, (b) 19 January 1999 at 12 UT, (c) 20 March 1999 at 12 UT and (d) 15 December 1998 at 12 UT.

reconstructions are a valuable tool for diagnosing the limitations of Eulerian models, as already shown by many other studies, but this is a topic we do not wish to dwell further in this study.

In the four cases shown in Figure 1, passively reconstructed profiles with 3D ECMWF winds show reasonable agreement with the observed profiles. They also exhibit sufficient amount of small-scale fluctuations over most of the profile, making them good candidates for estimating the vertical diffusion coefficients. Figure 2 shows the Payerne profile of 28 January 1999 and the 3D reconstructed profiles obtained without diffusion and with three different values of the diffusion coefficient, D=1., 0.1 and 0.01 $m^2s^{-1}$for a reconstruction time τ=15 days . From now on, we use N=1000 for the non-diffusive reconstructions and N=500 for the diffusive reconstructions.

By close examination of Figure 2, it is possible to see that the profile with $D = 0.1$ $m^2s^{-1}$is the most successful in eliminating the spurious laminae while at the same time preserving agreement with the smoothed non-diffusive profile and the observed profile. A more quantitative comparison is performed in Figure 3 showing the Fourier spectra of the diffusive ozone profiles and of the observed profile over the range of large to small scales. It is again clear that the best agreement in the spectra is for the case when $D = 0.1$ m^2s^{-1}.

A simple model of a laminated profile is obtained by assuming a chaotic advection of the tracer by the large-scale layerwise motion. This process generates a k^{-1} slope in the tracer spectrum which fits fairly well the spectrum for the non-diffusive reconstruction in Figure 3. The spectra for the observed profile and the diffusive reconstructions are steeper, with a tendency to fit a $k^{-5/3}$ slope for the observed profile. For the largest value of diffusion (D=1 m^2s^{-1}), the spurious effect of the discrete sampling of the white noise produces a flat spectrum at the smallest scales. The main source of vertical variance is the mean vertical ozone profile which does not show any noticeable evolution over the reconstruction period. Consequently, the spectra for the re-

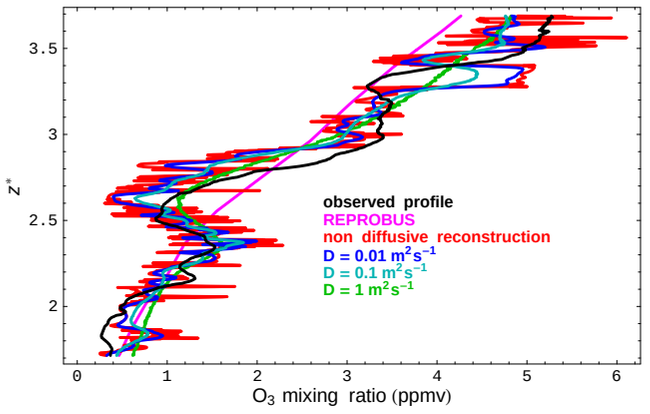

Figure 2. Ozone profiles at Payerne, 28 January 1999 at 12 UT, from ozonesonde, REPROBUS and 3D reconstruction without diffusion and with $D = 0.01$, 0.1 and 1 m^{2}s^{-1}. The vertical coordinate is $z^* = -\ln(p/p_0)$ with p_0=1000 hPa. The vertical scale runs between 180 and 25 hPa.

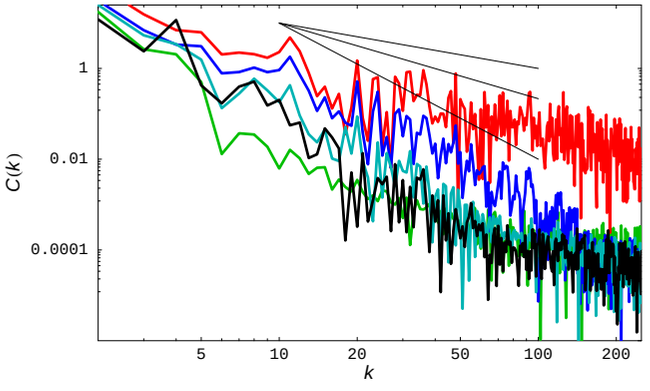

Figure 3. Comparisons of the Fourier spectra of the observed profile and that of three reconstructed profiles with different values of the vertical diffusion, for the profile at Payerne, on 28 January 1999 at 12 UT. Color coding as in Figure 2. For each profile, the spectrum is calculated after detrending by a linear fit. The straight lines indicate the slopes k^{-1}, $k^{-5/3}$ and k^{-3}.

constructed profiles can be considered as quasi-steady. Except at the smallest scales which are polluted as mentioned above, the variance of the detrended signal decreases as the diffusion increases. In the intermediate range ($5 < k < 100$) where spectra best separate, the observed spectra is compatible with both mid and high diffusion values and excludes the low diffusion value.

In order to bound the value of the vertical diffusivity still further, we present now the results of two other methods to analyze the reconstructed profiles.

Since we are discussing the effect of transport on the distribution of vertical fluctuations in the ozone mixing ratio, it would be particularly useful to compare the probability density functions (pdf) of vertical ozone increments in the observed and the reconstructed profiles. There is not enough data to provide a reliable estimate of these quantities and we can only compare simpler statistical estimates like the variance of the increment. Even then, there is too much noise in the small scales, in particular for the large diffusion case, to get significant results from raw data. Therefore, a moving average over 5 adjacent points in the profile (10 for the non-diffusive case; remember that the vertical resolution is doubled in this case) is applied prior to the calculation of the increments. The ozone increments are taken over adjacent points except for the non-diffusive case where they are taken over a distance of two points. These increments basically measure the local gradient of the profiles smoothed by the moving average.

Figure 4 shows the increment variance as a function of the reconstruction time. The variance keeps growing after 24 days in the non-diffusive case while it levels off for the diffusive cases after 10 to 15 days. The curves for $D = 0.1$ m^{2}s^{-1}converge to a value close to the increment variance of the observed profile. Using a conservative estimate of a few tens of degrees of freedom in the profiles, a standard statistical F-test rejects variance ratios which are of the order of 2 or larger but does not reject a ratio 1.3. Therefore, both the small and the large value of diffusion are rejected. Similar results are obtained by repeating the same calculations using the mean absolute deviation instead of the variance (not shown).

The spectral comparison emphasizes the differences due to largest scale fluctuations in the profile while the increment variance emphasizes the small-scale fluctuations. What we really need, in order to conclude two curves are alike, is a definition of roughness (or rugosity) spanning the whole

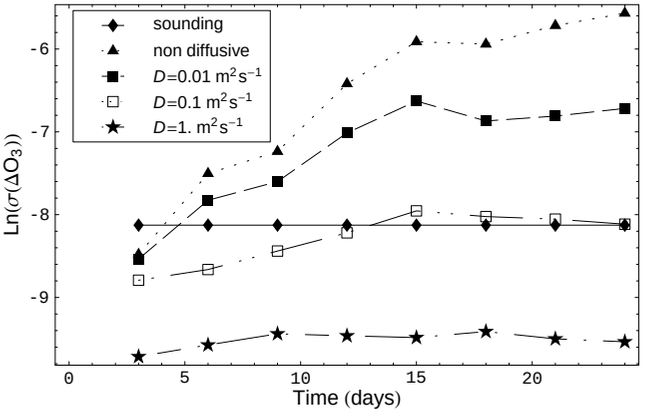

Figure 4. Variance of the ozone increment between two neighbouring points of the profile as a function of reconstruction time.

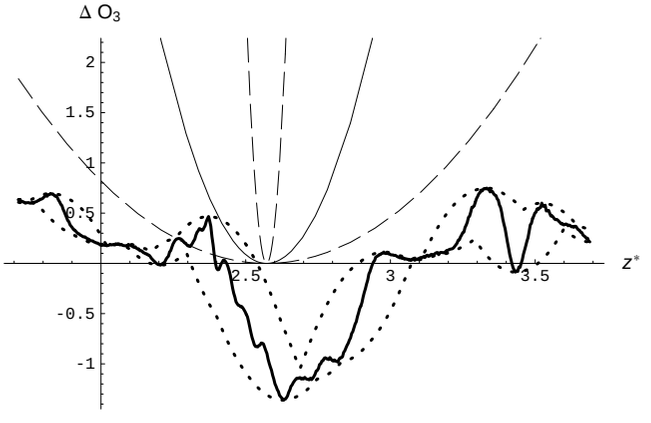

Figure 5. Sketch of the roughness measure. Heavy solid: an ozone profile as a function of log-pressure. Thin solid: the osculating parabola. Dot: the two osculating curves. Dash: the two extreme parabola corresponding to largest and smallest p in this study.

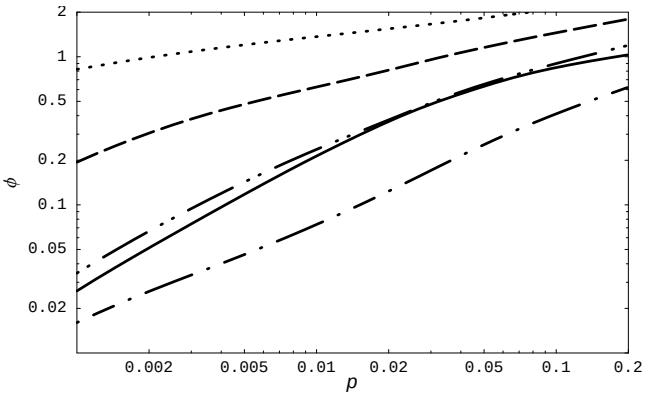

Figure 6. Roughness as a function of the parabola parameter p in Payerne on 28 January 1999, 12 UT for 15-day reconstructions. —: observed profile; $\cdots$reconstruction; $--$: $D = 0.01\mathrm{m}^2\mathrm{s}^{-1}$; $-\cdot\cdot$: $D = 0.1\mathrm{m}^2\mathrm{s}^{-1}$; $-\cdot-$: $D = 1\mathrm{m}^2\mathrm{s}^{-1}$. The parameter p is defined up to an arbitrary multiplicative factor.

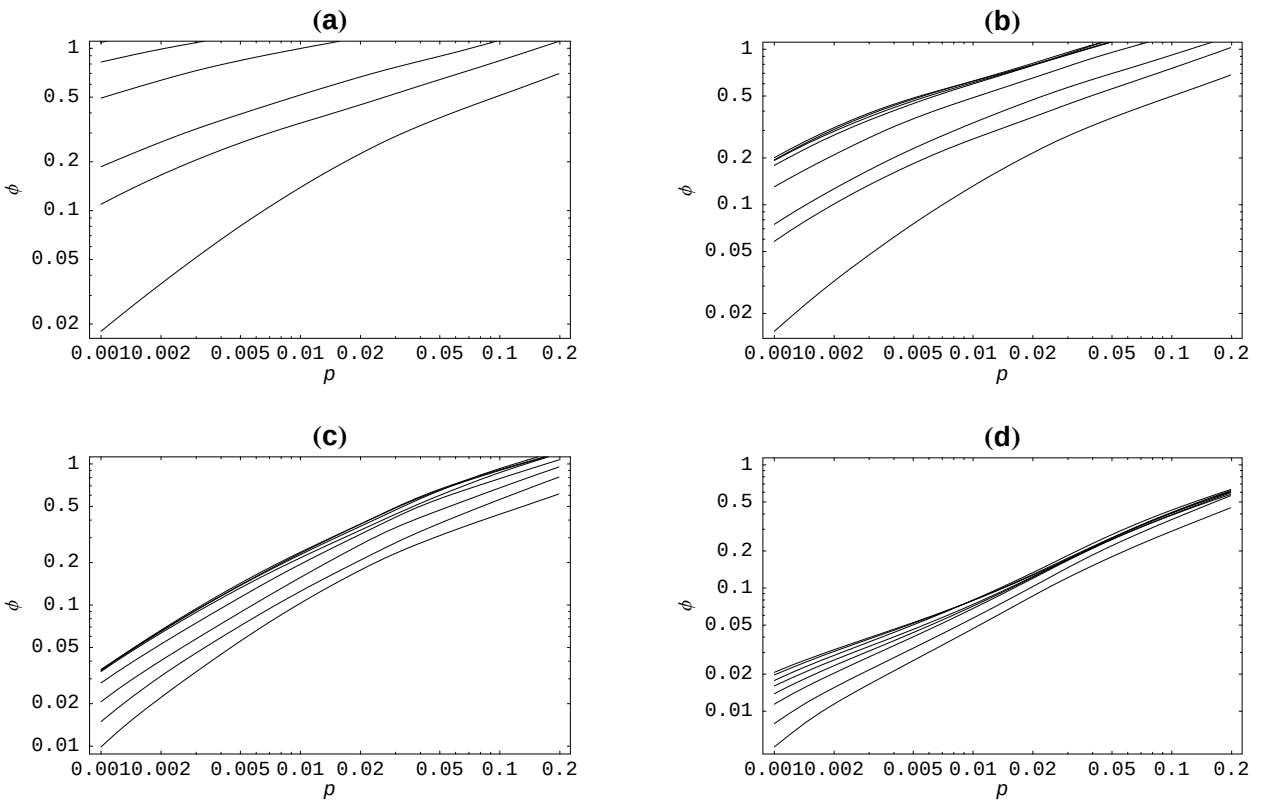

Figure 7. Roughness $\phi(p)$ for different reconstruction times. In each panel curves are ordered in increasing time from bottom to top. Shown times: 3, 6, 9, 12, 15, 18, 21 and 24 days. (a): non-diffusive case; (b): $D = 0.01$ m^{2}s^{-1}; (c): $D = 0.1$ m^{2}s^{-1}; (d): $D = 1$ m^{2}s^{-1}.

range of scales. For this purpose, we propose here a method inspired by image processing, where a common technique to filter contours is by rolling a virtual circle along them *Russ* [2002][see, e.g.,]. To apply this idea for smoothing a curve $y = f(x)$ requires the circle to be replaced by a parabola given by the equation

$$2p(y - y_c) = (x - x_c)^2. \quad (6)$$

The reason is that an arbitrary rescaling of the axis preserves the parabolic shape and is equivalent to multiplying p by a constant while a circle would be transformed into an ellipse under the same transformation. The algorithm then follows readily for a function $y = f(x)$ given by a list of N points (y_i, x_i) within an interval I.

1. For each value of $p > 0$ and for a given value $x_c = x_i$, one looks for $y_p^+(x_i)$ as the smallest y_c such that the parabola defined by (6) lies entirely above the curve joining the points (y_i, x_i).

2. Similarly, one defines $y_p^-(x_i)$ as the largest y_c such that the parabola defined by (6) with p changed into $-p$ lies entirely below the curve.

3. The two osculating curves $y_p^+(x_i)$ and $y_p^-(x_i)$ are then bracketing the discretized function $y = f(x)$. A measure of

roughness at scale p is defined by $\phi(p) = 1/N \sum_{i=1}^{N} (y_p^+(x_i) - y_p^-(x_i))^2$.

Figure 5 illustrates the bracketing of the reconstructed profile by the two osculating curves and shows the parabolas associated with largest and smallest p used in this study. The roughness function is basically the mean quadratic deviation between the two osculating curves.

Figure 6 shows the roughness function $\phi(p)$ calculated for the detrended observed and reconstructed profiles in Payerne on 28 January 1999 with 15-day reconstruction. The method is applied to detrended profiles. The five curves are well separated over more than two decades in p. Though the reconstructed curves exhibit less curvature than for the sounding, a fairly good fit to the sounding is provided by the diffusive reconstruction with D=0.1 m^{2}s^{-1}. The effect of particle noise shows up in the large diffusion case as an inflection and a flattening for small p. Figure 8(b) shows the roughness function obtained after smoothing by the same moving average as earlier for the calculation of the increment. The values of ϕ for small p are reduced with respect to the unfiltered case and the inflection of the large diffusion curve has disappeared. The separation of the curves is enhanced and D=0.1 m^{2}s^{-1}provides an excellent fit to the sounding.

Figure 7 shows the roughness curves as a function of the reconstruction time for the same case as in Figure 6. There is no convergence for the non-diffusive case. This is expected since chaotic dynamics induces irreversible separation of neighbouring particles. All the other curves converge after 10 to 15 days like for the variance increment, except for the small p values in the large diffusion case where the particle noise is increasing with time.

Figure 8 shows the roughness calculated for the four selected soundings after smoothing of all curves as mentionaed earlier. In Payerne on 29 March 1999, D =0.1 m^{2}s^{-1}still provides an excellent fit to the sounding while the two other cases suggest a slightly larger value for D, especially for Legionowo on 23 December 1998. All cases exclude, however, values as large as D=1 m^{2}s^{-1}. Also shown in Figure 8(b) is the result of a calculation where we have used a horizontal diffusion D_H = 6000 m^{2}s^{-1}instead of a vertical diffusion. The position of this curve among the others is compatible with the estimate of 0.1 m^{2}s^{-1}for the vertical diffusivity and an aspect ratio of horizontal versus vertical structures of the order of 250 [*Waugh et al.*, 1997].

Finally, we investigate the sensitivity of our results to the spatial resolution of the wind data. Figure 9(a) compares the reconstructed profile in Payerne on 29 March 1999 with that obtained using T319 wind data and a half-degree grid. The diffusion is $D = 0.1$m^{2}s^{-1}in both cases. The difference between the two profiles is small at all levels and impacts very slightly on the rugosity as shown by the curve corresponding to the high-resolution case in Figure 8(c). This result is in fair agreement with previous findings that transport in the lower stratosphere is dominated by the large scales of the flow [*Waugh and Plumb*, 1994; *Methven and*

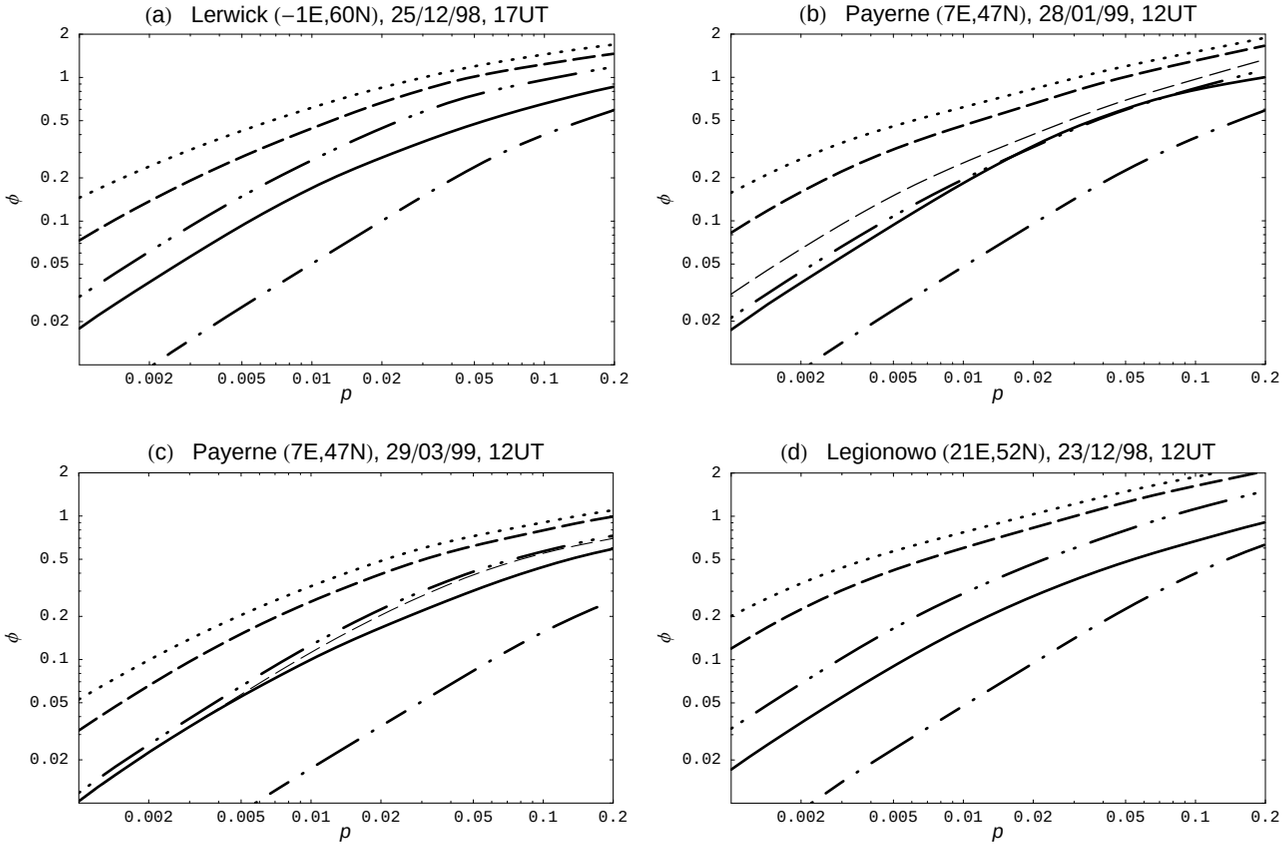

Figure 8. Roughness curves $\phi(p)$ for the four selected soundings. (a) in Lerwick, on 25 December 1998, 17 UT, for 12.25-day reconstructions; (b) in Payerne, on 28 January 1999, 12 UT for 15-day reconstructions; (c) in Payerne, on 29 March 1999, 12 UT for 12-day reconstructions; (d) in Legionowo, on 23 December 1998, 12 UT for 12-day reconstructions. Curves as in Figure6 except in (b) where the thin dash curve is for the reconstruction with horizontal diffusion D_H = 6000 m^{2}s^{-1}and in (c) where the thin dashed curve is for the reconstruction with high-resolution wind presented in Figure 9.

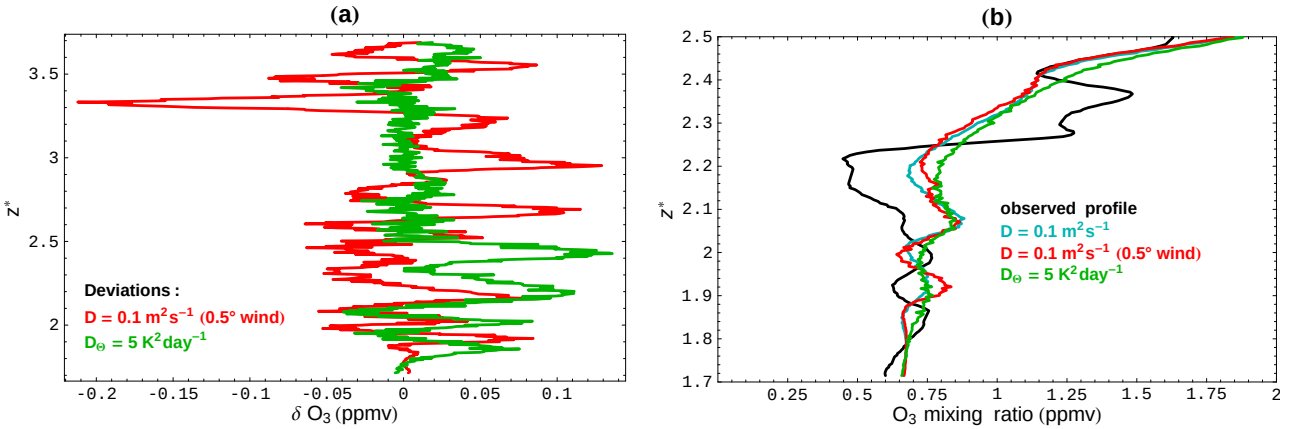

Figure 9. Comparison of the reconstructed profiles in Payerne on 29 March 1999. The reference reconstruction is that obtained using $D = 0.1\mathrm{m}^2\mathrm{s}^{-1}$for 12-day reconstructions. (a) Deviations to the reference of the reconstruction obtained with high-resolution (0.5°) wind and of the reconstruction obtained with $D_\theta = 5\mathrm{K}^2\mathrm{day}^{-1}$. (b) Lower part of the observed profile and the reconstructed profiles as indicated in the legend.

Hoskins, 1999]. Figure 9(a) also shows the deviation of the reconstructed curve obtained with a diffusion in potential temperature D_Θ=5 $\mathrm{K}^2\mathrm{day}^{-1}$using (5). This value is obtained from D=0.1 $\mathrm{m}^2\mathrm{s}^{-1}$by assuming a potential lapse rate $d\theta/dz$ = 24 K km^{-1} in the lower stratosphere. It is seen that the deviation is extremely small above z^* = 2.5 or p = 82hPa. Below this altitude, the deviation is still small but increases abruptly. Figure 9(b) shows that the reconstructed profile with D_Θ=5 $\mathrm{K}^2\mathrm{day}^{-1}$is much smoother than that obtained with D=0.1 $\mathrm{m}^2\mathrm{s}^{-1}$indicating that this region favors vertical mixing in θ. Indeed, the vertical stability $d\theta/dz^*$ is not fixed but increases with height in the stratosphere. It is, however, surprising to see such a sharp transition, above and below z^* = 2.5, in the diffusive properties, despite the facts that neither does vertical stability exhibit such a transition nor do back-trajectories show any noticeable separation over more than 8 days of the reconstruction (not shown).

4. Discussion

We have presented a set of simple techniques to estimate vertical diffusion coefficient from balloon ozone soundings in the lower stratosphere. We find that $D \approx 0.1\mathrm{m}^2\mathrm{s}^{-1}$or slightly larger provides a good fit between our reconstructed curves and the observed ozone profiles for a small set of selected soundings during the northern hemisphere winter. As we are limited by the resolution of ozone soundings which smears out fluctuations with vertical scales of less than about 100m, our estimate is an upper bound on the actual diffusivity.

The most relevant earlier study to compare our estimates of D seems to be that of *Balluch and Haynes* [1997], which provides estimates based on tracer data and simulations over a period of 2 weeks or so. Those estimates are of the order of 10^{-2} $\mathrm{m}^2\mathrm{s}^{-1}$or even lesser. As noted by these authors, the processes that cause the vertical diffusion are attributed to the combined effects of mixing by turbulent motion, and large-scale horizontal stirring plus large-scale vertical shear, causing diffusion to be more effective in the vertical. These effects are also relevant in the context of our study, done over a period of 12 days or so. However, the above study is based on the analysis of the isentropic deformation of single filaments reduced to a simplifying one-dimensional approximation and exhibit large variations of the estimated diffusivity (between 0.1 $\mathrm{m}^2\mathrm{s}^{-1}$and 0.001 $\mathrm{m}^2\mathrm{s}^{-1}$) from case to case. In contrast, it is the advection by the more realistic ECMWF three-dimensional winds that is utilized in the present study, and the only basic premise is that it is diffusion, which acts primarily in the vertical [cf. *Dewan*, 1981; *Haynes and Anglade*, 1997; *Alisse et al.*, 2000; *Vanneste and Haynes*, 2000], that is causing the relaxation of noisy ozone profile, reconstructed from individual trajectories, toward the observed one. The present results may be considered as representative of the overall effect of many effectively vertical mixing processes, on a time scale of 1 to 2 weeks. However, it is likely that, because of the qualitatively different nature of flow regimes in different parts of the stratosphere at different times of the year, one may need to estimate flow dependent values of D that also agree with tracer observations in the specific period and region of interest.

Our estimate of D based on 3D calculations is larger than that reported in *Balluch and Haynes* [1997], but the two results are compatible since we can only provide an upper bound. The present estimate is an order of magnitude less than estimates, valid over a few hours, based on early radar observations [cf. *Fukao et al.*, 1994, and references therein] and numerical calculations based on individual dynamical events [*Schilling and Jenssen*, 1992].

Historically, there is a large number of available ozone soundings distributed around the globe. Hence, it seems feasible to repeat the present study over a large dataset to investigate circulation-dependent spatial-temporal statistics of D in the stratosphere. On the other hand, the reduced set of high-resolution soundings or aircraft data in the stratosphere gives access to vertical resolution or equivalent vertical resolution much smaller than the standard ozone sounding and allows to investigate further the upper bound on effective diffusivity.

Acknowledgments. BJ thanks the support of European Community grant ENV4-CT97-0520. The trajectory calculation have been done with a code based on FLEXPART provided by Andreas Stohl. We thank Vincent Daniel for providing helpful advice and guidance on FLEXPART and an anonymous reviewer for his remarks that led to improvement of the manuscript.

Notes

1. We use ECMWF analysis which is available at 6-hour interval during this period and 3-hour forecasts for the other times.
2. The vertical velocity is computed by the FLEXPART preprocessor using a mass conserving scheme in the hybrid ECMWF coordinates.

References

Akima, H., A method of univariate interpolation that has the accuracy of a third-oder polynomial, *ACM Trans. Math. Soft.*, *17*, 341–366, 1991.

Alisse, J.-R., P. Haynes, J. Vanneste, and C. Sidi, Quantification of stratospheric mixing from turbulence microstructure measurements, *Geophys. Res. Lett.*, *27*, 2621–3224, 2000.

Balluch, M., and P. Haynes, Quantification of lower stratospheric mixing processes using aircraft data, *J. Geophys. Res.*, *102*, 23,487–23,504, 1997.

Bhatt, E. E., P. P.and Remsberg, L. L. Gordley, J. M. McInerney, V. G. Brackett, and J. M. Russell III, An evaluation of the quality of HALOE ozone profiles in the lower stratosphere, *J. Geophys. Res.*, *D104*, 9261–9275, 1999.

Dewan, E., Turbulent vertical transport due to thin intermittent mixing layers in the stratosphere and other stable fluids, *Science*, *211*, 1041–1042, 1981.

Dole, J., and R. Wilson, Estimates of turbulent parameters in the lower stratosphere - upper troposphere by radar observations: A novel twist, *Geophys. Res. Lett.*, *27*, 2625–2628, 2000.

Fukao, S., M. Yamanaka, N. Ao, W. Hocking, T. Sato, M. Yamamoto, T. Nakamura, T. T., and S. Kato, Seasonal variability of vertical eddy diffusivity in the middle atmosphere. Three-year observations by the middle and upper atmosphere radar, *J. Geophys. Res.*, *99*, 18,973–18,987, 1994.

Haynes, P., and J. Anglade, The vertical-scale cascade of atmospheric tracers due to large-scale differential advection, *J. Atmos. Sci.*, *54*, 1121–1136, 1997.

James, P., A. Stohl, S. Forster, S. Eckhardt, P. Seibert, and A. Frank, A 15-year climatology of stratosphere-troposphere exchange with a Lagrangian particle dispersion model, Part A: Methodology and mean climate, *J. Geophys. Res.*, p. in press, 2002.

Lefèvre, F., G. P. Brasseur, I. Folkins, A. K. Smith, and P. Simon, Chemistry of the 1991-1992 stratospheric winter: Three-dimensional model simulations, *J. Geophys. Res.*, *99*, 8183–8195, 1994.

Lefèvre, F., F. Figarol, K. Carslaw, and T. Peter, The 1997 Arctic ozone depletion quantified from three-dimensional model simulations, *Geophys. Res. Lett.*, *25*, 2425–2428, 1998.

Lucke, R., et al., The polar ozone and aerosol measurement (POAM III) instrument and early validation results, *J. Geophys. Res.*, *104*, 18,785–18,799, 1999.

Manney, G., W. Lahoz, R. Swinbank, A. O'Neill, P. Connew, and R. Zurek, Simulation of the December 1998 stratospheric major warming, *Geophys. Res. Lett.*, *26*, 2733–2736, 1999.

Mariotti, A., M. Moustaoui, B. Legras, and H. Teitelbaum, Comparison between vertical ozone soundings and reconstructed potential vorticity maps by contour advection with surgery, *J. Geophys. Res.*, *102*, 6131–6142, 1997.

Methven, J., and B. Hoskins, The advection of high-resolution tracers by low-resolution winds, *J. Atmos. Sci.*, *56*, 3262–3285, 1999.

Millard, G., A. Lee, and J. Pyle, A model study of the connection between polar and mid-latitude ozone loss in the northern hemisphere lower stratosphere, *J. Geophys. Res.*, p. to appear, 2002.

Morikawa, G., and E. Swenson, Interacting motion of rectilinear geostrophic vortices, *Phys. Fluids*, *14*, 1058–1073, 1971.

Nastrom, G., and F. Eaton, Turbulent eddy dissipation rates from radar observations at 5-20 km at White Sand missile range: New Mexico, *J. Geophys. Res.*, *102*, 19,495–19,505, 1997.

Orsolini, Y., On the formation of ozone laminae at the edge of the Arctic polar vortex, *Quart. J. Roy. Met. Soc.*, *121*, 1923–1941, 1995.

Orsolini, Y., G. Hansen, G. Manney, N. Livesey, and U.-P. Hoppe, Lagrangian reconstruction of ozone column and profile at the Arctic Lidar Observatory for Middle Atmosphere Research (ALOMAR) throughout the winter and spring of 1997-1998, *J. Geophys. Res.*, *106*, 10,011–10,021, 2001.

European Ozone Research Coordinating Unit, The northern-hemisphere stratosphere in the winter of 1998-1999, *Tech. rep.*, Directorate-General XII, Science, Research and Development, 1999.

Richardson, L., Atmospheric diffusion shown on a distance-neighbour graph, *Phil. Trans. R. Soc. London A*, *110*, 709–737, 1926.

Russ, J., *The Image Processing Handbook*, CRC Press, 2002.

Schilling, V., and D. Etling, Vertical mixing of passive scalars owing to breaking gravity waves, *Dyn. Atmos. Oceans*, *23*, 371–378, 1996.

Schilling, V., and U. Jenssen, Particle dispersion due to dynamical instabilities in the lower stratosphere, *Contrib. Atmos. Phys.*, *65*, 259–273, 1992.

Sparling, L., J. Kettleborough, P. Haynes, M. McIntyre, J. Rosenfield, M. Schoeberl, and P. Newman, Diabatic cross-isentropic dispersion in the lower stratosphere, *J. Geophys. Res.*, *102*, 25,817–25,829, 1997.

Stohl, A., S. Eckhardt, C. Forster, P. James, N. Spichtinger, and P. Seibert, A replacement of simple back trajectory calculations in the interpretation of atmospheric trace substance measurements, *Atmos. Environn.*, *36*, 4635–4648, 2002.

Sutton, R., H. Maclean, R. Swinbank, A. O'Neill, and F. Taylor, High-resolution stratospheric tracer fields estimated from satellite observations using Lagrangian trajectory calculations, *J. Atmos. Sci.*, *51*, 2995–3005, 1994.

Taylor, G., Diffusion by continuous movement, *Proc. London Math. Soc.*, *20*, 196–212, 1921.

Vanneste, J., and P. Haynes, Intermittent mixing in strongly stratified fluids as a random walk, *J. Fluid Mech.*, *411*, 162–185, 2000.

Waugh, D., and R. Plumb, Contour advection with surgery: A technique for investigating fine scale structure in tracer transport, *J. Atmos. Sci.*, *51*, 530–540, 1994.

Waugh, D., et al., Transport of material out of the stratospheric Arctic vortex by Rossby wave breaking, *J. Geophys. Res.*, *99*, 1071–1088, 1994.

Waugh, D., et al., Mixing of polar air into middle latitudes as revealed by tracer-tracer scatter plots, *J. Geophys. Res.*, *102*, 13,119–13,134, 1997.

Williamson, D. L., Semi-Lagrangian moisture transport in the NMC spectral model, *Tellus*, *42A*, 413–428, 1989.

Woodman, R., and P. Rastogi, Evaluation of effective eddy diffusive coefficients using radar observations of turbulence in the stratosphere, *Geophys. Res. Lett.*, *11*, 243–246, 1984.

Zouari, N., and A. Babiano, Derivation of the relative dispersion law in the inverse energy cascade of two-dimensional turbulence, *Physica D*, *76*, 318–328, 1994.

Bernard Legras, Laboratoire de Météorologie Dynamique (UMR 8539), Ecole Normale Supérieure, 24 Rue Lhomond, 75231 Paris Cedex 05, France. (e-mail: legras@lmd.ens.fr)

Binson Joseph, Department of Mathematics, Arizona State University, P.O. Box 871804, Tempe, AZ 85287-1804, USA (e-mail: binson@math.la.asu.edu)

Franck Lefèvre, Service d'Aéronomie (UMR 7620), Université Pierre et Marie Curie, Tour 15 - 5ème étage, case 102, 4 Place Jussieu, 75252 Paris Cedex 05, France. (e-mail: franck.lefevre@aero.jussieu.fr)

(Received _____.)